

# Structural Damage Localization in a Suspension Bridge Under Seismic Excitation



**M. Domaneschi, M.P. Limongelli & L. Martinelli**

*Politecnico di Milano, Department of Structural Engineering, Milan, Italy*

## SUMMARY:

In this paper we present the application of the Interpolation Damage Detection Method (IDDM) to the numerical model of a suspension bridge having a long span truss-stiffened deck. The method, which belongs to Level II damage identification method, can identify the presence and the location of a damage based on acceleration responses of the structure before and after a damaging event without explicit knowledge of the modal properties of the structure.

Emphasis is placed on the influence of noise in recorded signals on the reliability of the results given by the IDDM method. The response of the suspension bridge to seismic excitation is computed from the model and artificially corrupted with random noise characteristic of two families of MEMS accelerometers, in order to simulate real conditions. The reliability of the results has been checked for different damage scenarios.

*Keywords: Damage detection, Suspension Bridges, MEMS, noise*

## 1. INTRODUCTION

Health monitoring of long span bridges using vibration techniques have recently received an increasing attention as efficient alternative to visual inspection in order to detect damage.

Among the damage detection methods proposed in literature, herein the Interpolation Damage Detection Method (IDDM), which has been recently proposed and applied to damage detection of wind excited structures (Domaneschi et al. 2011) is selected. The damage identification method IDDM (Interpolation Damage Detection Method) is applied to a numerical model of a suspension bridge, derived from the design data of the Shimotsui–Seto bridge (JP), having a long span (940 m) truss-stiffened deck and loaded by earthquake excitation.

The IDDM method belongs to the ones based on deformed shapes of the structure which appear very promising for damage localization (Pandey 1991, Sampaio 1999, Ratcliffe 2000). The method can identify the presence and the location of a damage based on the accelerometric responses recorded on the structure before and after a damaging event, and does not require the explicit knowledge of the principal modes of the structure, nor of the damaged structure, thus eliminating the need to identify and validate the corresponding modal parameters and shapes. The advantage of the method is the modest computational burden required and its capability to be used without human intervention. This makes it promising for future use in on-line monitoring systems which are particularly useful for strategic structures such as road infrastructures.

In this paper emphasis is placed on the influence of noise, present in the recorded signals, on the reliability of results given by the IDDM method. The response of the suspension bridge subjected to seismic excitations, is computed in the framework of the ANSYS finite element environment and responses are calculated on the model at different location along the bridge deck. These signals are artificially corrupted with random noise in order to simulate real operational conditions. The reliability of the results has been checked for different damage scenarios, characterized by different location of the damage. This was simulated by a reduction of stiffness in different position of the deck. Results

show the reliability of the method with respect to (a) the correct localization of damage in all the considered scenarios; (b) the capability to detect damage using earthquakes of low intensity in the identification procedure; (c) the correlation between the level of noise and the results.

## 2. SUSPENSION BRIDGE GEOMETRY AND NUMERICAL MODEL

The suspension bridge herein considered as object of the damage detection exercise is the Shimotsui-Seto bridge (Domaneschi and Martinelli 2011), located in Japan. It spans from the side of Mt. Washu to the Hitsuishijima Island and has of a single span stiffened truss deck. Figure 2.1 shows the main characteristics of the bridge.

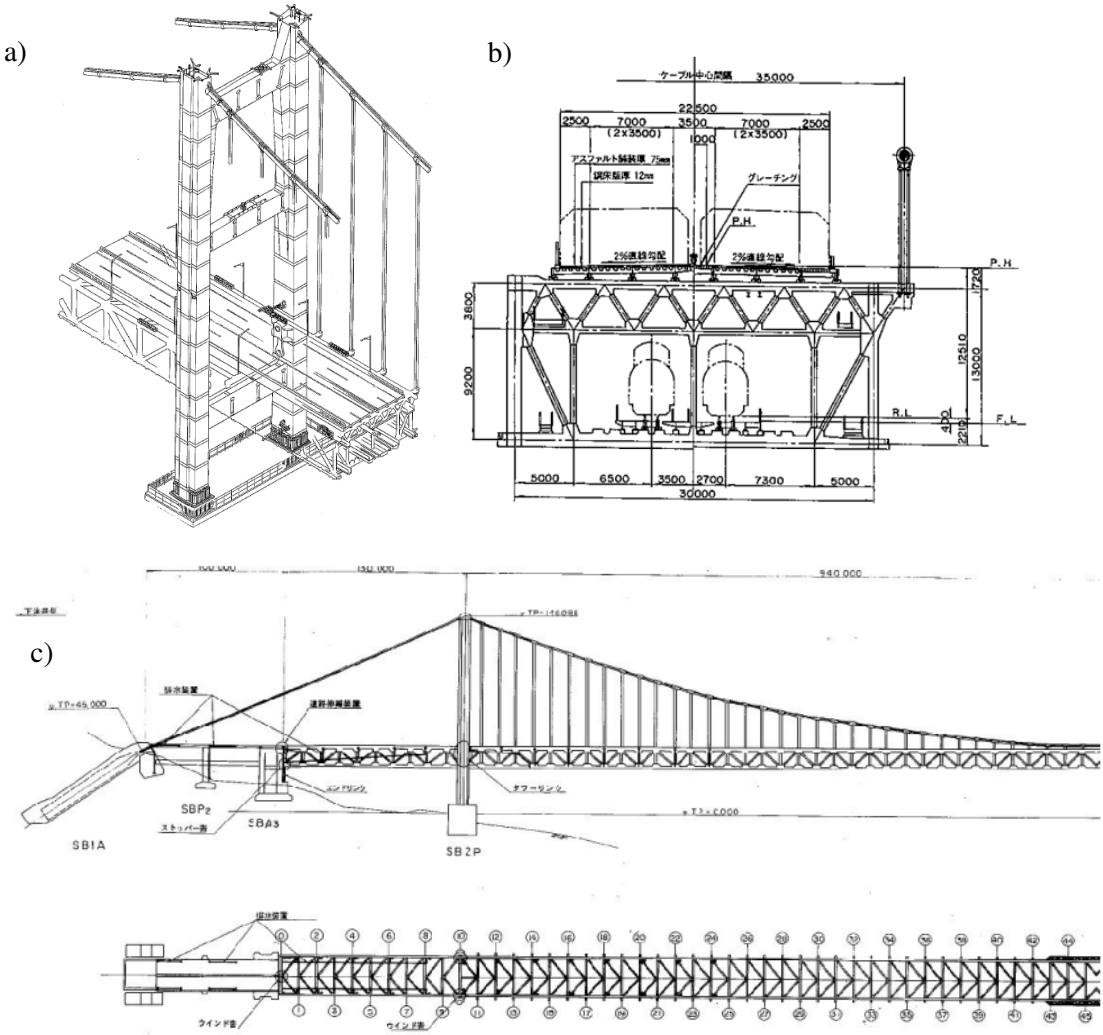


**Figure 2.1.** Bridge geometry: (a) tower detail; (b) deck transversal section; (c) general dimensions. Courtesy of Mr. M. Nishitani HBSE-JP.

The main geometric dimensions of the structure are: length, 1400 m (940 m the main span), excluding 46 m-girder on anchorage; towers height, 149 m; vertical distance of the main girder from the towers foundation, 31 m; main girder of section 30x13 m (width and thickness, respectively). The main cables, the hangers and the main girder are in steel while the towers are assumed as built in concrete (Romano 2009).

Two numerical models of the suspension bridge have been developed in the ANSYS framework. These are characterized by different refinement levels (Domaneschi and Martinelli 2011). A first,

detailed, model (Figure 2.2a), implements a almost one-to-one correspondence between structural and Finite Elements (FE). Its geometrical and mechanical properties have been assessed by matching the first four natural periods and modal shapes with those measured on the real structure.

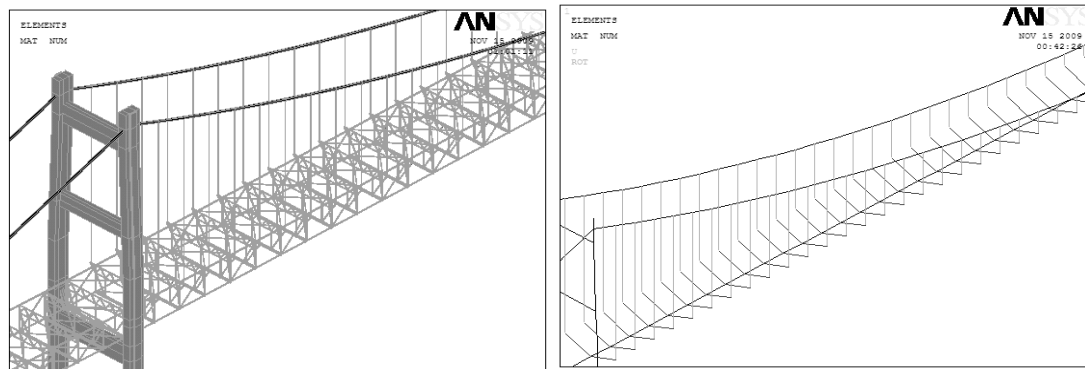


**Figure 2.2.** Detailed bridge model with a one-to-one member to F.E. correspondence (a). Simplified bridge model for time-histories numerical analyses (b).

Initially, a preliminary linear static analysis was conducted on this bridge model, considering as load only the weight of the structural elements. The displacement field thus obtained was used to correct the position of the nodes in the initial non-deformed configuration by displacing the nodes of an amount equal to the movement predicted by the static analysis. The configuration of the bridge, obtained in this way, coincides with the design one and takes into account the state of stress induced by the mass density.

A simplified model (Figure 2.2b), more manageable for the numerically full integrated non linear transient analyses in ANSYS, was subsequently derived and validated by the application of the Modal Assurance Criterion (Allemang and Brown 1982).

### 3. IDDM DAMAGE DETECTION PROCEDURE

The method applied to detect and localize damage is the Interpolation Damage Detection Method (IDDM) previously presented in (Limongelli 2009, 2010, 2011) for the case of seismically excited structures.

The damage detecting feature is defined in terms of the error related to the use of a spline function in modelling the deformed configuration of the bridge. Specifically, at a given location the modelling accuracy is defined as the difference between the measured displacement and the displacement computed at that same location interpolating through a proper function the displacements measured at all the other locations equipped with a sensor. The basic assumption is that if the comparison between the interpolation error in the baseline phase on the undamaged structure and in the inspection phase on the potentially damaged structure shows that there is a significant decrease of accuracy, this is an indication of the existence of damage at a location close to the one where this change is detected.

The method is applied to the case of structures subjected to a seismic excitation by defining the interpolation error at a given location in terms of the transfer functions of the absolute acceleration at that location with respect to the base input.

The transfer functions between the acceleration at the base and the absolute acceleration of the points of the structure provide the "Operational Modal Shapes" (OMS) at the generic frequency and the modal shapes (MS) in correspondence of the modal frequencies.

See Figure 3.1 for a representation of such functions, computed for the signals recorded at the measurement positions  $z_i$ .

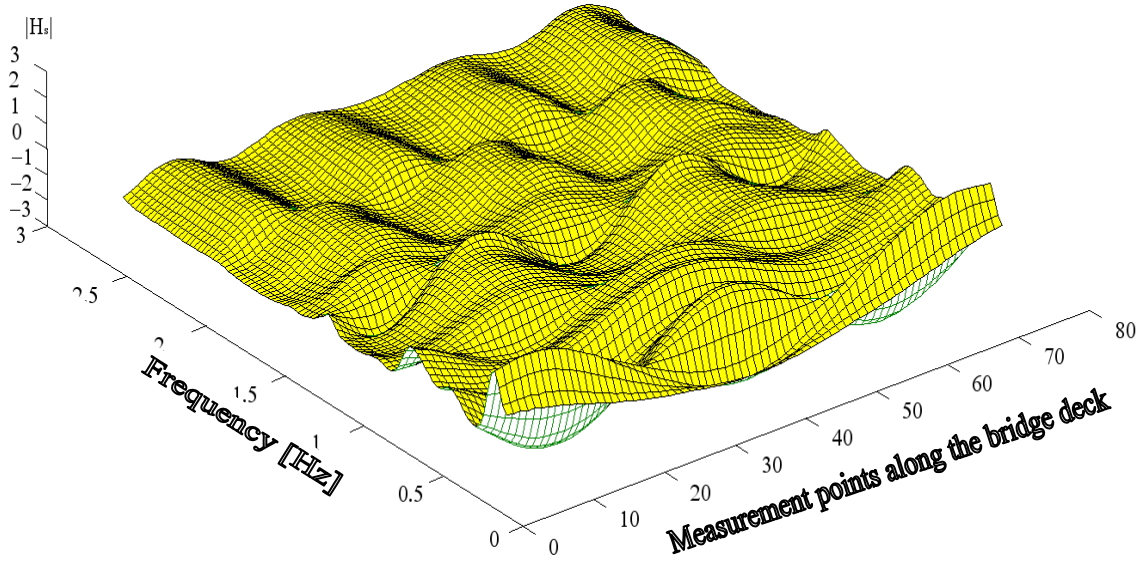


**Figure 3.1.** Modulus of the transfer functions  $H_R(z_i, f)$  for displacements in direction normal to the bridge axis for stations from 1 to 71 and for frequencies from 0 to 2,5Hz..

The spline interpolation error is defined as the difference, calculated over the entire frequency range in which the signal-to-noise ratio is significant, of the transfer functions obtained from the recorded signals with respect to those calculated by the interpolated signals.

Use of transfer functions allows to eliminate the influence of the excitation amplitude and frequency content on the error function.

At each frequency  $f$ , the transfer function  $H_S(z_l, f)$  between input and output in the  $l$ -th measurement position at  $z_l$  may be computed by spline interpolation of transfer functions  $H_R(z_i, f)$  at frequency  $f$ .

$$H_S(z_l, f) = \sum_{j=0}^3 c_{j,l}(f)(z_l - z_{l-1})^j \quad (3.1)$$

where the coefficients ( $c_{0l}, c_{1l}, c_{2l}, c_{3l}$ ) are functions of the  $H_R(z_k, f)$  at the other locations:

$$c_{j,l}(f_i) = g(H_R(z_k, f_i)) \quad k \neq l \quad (3.2)$$

The interpolation error at location  $z$  (in the following the index  $l$  will be dropped for clarity of notation) at the  $i$ -th frequency value  $f_i$ , is defined as the difference between the magnitudes of recorded and interpolated transfer functions:

$$\Delta H(z, f_i) = |H_R(z, f_i)| - |H_S(z, f_i)| \quad (3.3)$$

where  $H_R$  is the transfer function of the response recorded at location  $z$  and  $H_S$  is the spline interpolation at  $z$ . In order to characterize each location with a single error parameter, the norm of the error on the whole range of frequencies has been considered:

$$E(z) = \sum_{i=1}^N \sqrt{\Delta H^2(z, f_i)} \quad (3.4)$$

$N$  is the number of frequency lines in the transfer functions correspondent to the frequency range where the signal-to-noise ratio is high enough to allow a correct definition of the transfer function.

The values of the transfer function depends on the state of the structure, hence if the estimation of the error function through Eqn. (3.4) is repeated in the baseline (undamaged) and in the inspection (potentially damaged) phases, the comparison between the two values, respectively  $E_0$  and  $E_d$  should give an indication about the existence of damage at the considered location.

$$\Delta E(z) = E_d(z) - E_o(z) \quad (3.5)$$

An increase of the interpolation error between a reference and the current configuration points out a variation of the operational deformed shape hence a variation of stiffness associated with damage. In order to remove the effect of random variations of  $\Delta E$  and assuming a Normal distribution of this function, the 98% percentile is assumed as a minimum value beyond which no damage is considered at that location. In other words a given location is considered close to a damaged portion of the structure if the variation of the interpolation error exceeds the threshold calculated in terms of the mean  $\mu_{\Delta E}$  and variance  $\sigma_{\Delta E}$  of the damage parameter  $\Delta E$  on the population of available records that is:

$$\Delta E(z) > \mu_{\Delta E} + 2\sigma_{\Delta E} \quad (3.6)$$

The damage index is then defined by the relation:

$$D(z) = \Delta E(z) - (\mu_{\Delta E} + 2\sigma_{\Delta E}) \quad (3.7)$$

## 4. EARTHQUAKE LOADING AND DAMAGE SCENARIOS

### 4.1. Earthquake loading

Earthquake loading is applied at the support point of the bridge (base of towers and bents) in the form of synchronous fully 3-Dimensional acceleration time histories of natural events. The seven events selected for this study are listed in Table 4.1. These records have all been scaled to a Peak Ground Acceleration (PGA) of 0.175 g to simulate the acquisition of information from earthquakes relatively common during the expected life of the structure, not great intensity, not likely to induce damage to the structure.

**Table 4.1.** Events selected for the characterization of the pristine structure

Event	Station	Source
Chalfant Valley 1986/07/21 14:42	54428 Zack Brothers Ranch	CDMG
Chi-Chi, Taiwan 1999/09/20	TCU072	CWB
Imperial Valley 1979/10/15 23:16	952 El Centro	USGS
Kobe 1995/01/16 20:46	0 Nishi-Akashi	CUE
Erzincan, Turkey 1992/03/13	95 Erzincan	---
Northridge 1994/01/17 12:31	90057 Canyon Country – W Lost Cany	USC
Loma Prieta 1989/10/18 00:05	47125 Capitola	CDMG

### 4.2. Instrumentation

The bridge has been assumed to be instrumented with unidirectional MEMS accelerometers located on the deck at each node of the finite element model, recording transversal horizontal accelerations. The nodes of the deck central span, see Figure 4.1, are numbered from N1 to N71 with node N36 at the deck mid-span. The IDDM method is applied first to the undamaged structure and then on the damaged one.

It is well known that MEMS accelerometric sensors can be very economic; at the same time economic MEM sensors are known for the high level of sensor noise. Whenever they are of high quality their cost per channel is comparable to that of other technologies (e.g. of servo-accelerometers). Since emphasis is on noise effects, MEMS sensors of different quality and costs, with two order of magnitudes difference, have been simulated by adding to the signals collected on the numerical models an appropriate white noise of intensity related to the noise density level characteristic of the two MEMS families herein considered.

The first family is representative of sensors (denoted as HN “High Noise” in the following) with a cost in the order of few euro per channel, developed for cellular phones applications or automotive one, statistically mass calibrated at the factory.

To this family it has been assigned a noise density of  $30\mu\text{g}/\sqrt{\text{Hz}}$  representative of an average noise values for sensors with a measuring range of  $\pm 2$  g. The second family is representative of MEM sensors of a higher class (denoted as LN “Low Noise” in the following), specifically developed for seismological applications, with a noise density of  $500\text{ng}/\sqrt{\text{Hz}}$  and a cost per channel in the order of  $10^2$  euro. For both sensors the bandwidth assumed has been 100 Hz, since the simulated sampling frequency in the numerical model was of 200 Hz.

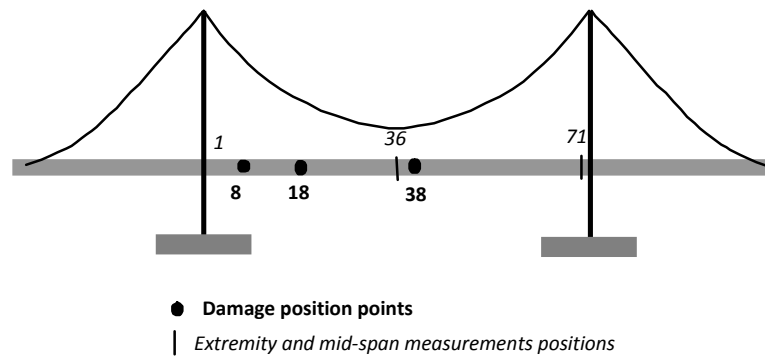


**Figure 4.1.** Location of acceleration measurements points.

### 4.3. Damage scenarios

The spline interpolation error in the reference configuration  $E_o(z)$  is calculated for both HN and LN sensors using the response to each of the seven natural accelerograms reported in Table 4.1.

The damaged structure was tested with only one signal Kobe 01/16/1995, again scaled to a PGA of 0.175 g to simulate the acquisition from an earthquake of low intensity, or an after-shocks of a strong event responsible for the damage.

The IDDM method of identification and location of the damage has been tested using a damage level similar to values already used in previous works of literature (Kho and Dyke 2007, Ntotsios et al. 2009).

In particular, the damage was simulated by a reduction of 30% and 50% of the elastic modulus of two elements at different points along the main girder to create different damage scenarios and test the sensitivity of the method to the position of the damage.

The denomination of the damage scenario indicates the node number where converge the two damaged beams and the amount of stiffness reduction, so that N18\_30% means a 30% reduction of the stiffness of the beams converging to node 18 in the simplified model of Figure 2.2b.

The following damage scenarios were investigated:

- a) damage at the point of measurement N8,
- b) damage at the point of measurement N18,
- c) damage at the point of measurement N38,

The measurement point N8 is close to the left tower while point N38 is next to the centreline of the bridge (see Figure 4.1).

## 5. RESULTS OF THE IDDM DAMAGE DETECTION METHOD

The results of running the IDDM identification procedure for the two sensors families (HN and LN), the four damage scenarios and the two damage levels (30% and 50%) considered in this work are summarized in Figures from 5.1 to 5.6. A comparison is shown between the values of the damage indicator parameter defined by Eqn. (3.5) using and the 2% fractile of the probability distribution of the variation  $\Delta E$ , which is the minimum value of the damage indicator in order to flag the corresponding node as close to a damaged section. The need to define a minimum value for the damage indicator appears clearly, since this response parameter takes values other than zero also in sections different from the damaged ones (the damage location is shown by a blue vertical line in the Figures), in addition to those actually damaged. Such circumstance can lead to a number of "false alarms", i.e. sections erroneously considered damaged, if the definition of the damage indicator is not made by considering the nature of the random variation of the interpolation error, and defining a lower threshold value bound at a given fractile of the damage indicator probability distribution.

A reduction of fractile value, to which an increase of the threshold value of the damage index is associated, would lead to a reduction of false alarm risk but, at the same time, to an increased risk of "missed" alarms related to the possibility that also in the section actually damaged the damage index does not exceed the threshold value. The choice of the minimum value of the damage index has to be the subject of a preliminary analysis, carried out on the structure so as to permit its determination on the basis of an acceptable compromise between the risk of having "false alarms" and of having "missed alarms".

All the computations of  $\Delta E$  are carried out using 50 frequency lines from  $H_R$  and  $H_S$ , starting from the 15th line, to reduce noise effects.

Figures 5.1-5.3 depict the performance of the procedure for the HN family of sensors and a damage value of 50%. Results for these sensors is clearly inadequate.

Changing the sensor family to the LN one brings a vast improvement. In Figures 5.4-5.6 the results for the smaller damage level (30%) are shown. The procedure shows good accuracy and efficiency, being able to correctly determine the location of the damage for all scenarios considered with a low computational cost associated with the processing of data relating to a single seismic event.

## 6 COMMENTS AND CONCLUSIONS

In this work we have verified applicability and performance of the IDDM damage identification method to the case of long span suspension bridges considering sensors noise. The method was applied to a numerical model of the Shimotsui-Seto bridge considering different scenarios of simulated damage. The effect of sensors noise is accounted for in the data used. The presence of noise induces random variations of the damage index and reduces the sensitivity of the method. Nevertheless, the results show that the method correctly provides the damage location, independently of the position, when high class MEMS sensors are used, while for the noisier more economic sensors, not specifically engineered for this type of applications, damage is correctly detected only when it induces a localized 50% stiffness reduction on the main girder and it is located near mid-span.

The main advantage of the method is the modest computational burden it requires and the possibility to be used in an automatic manner, without requiring interaction with an operator. This makes the method promising for future applications in on-line monitoring systems particularly useful in the case of strategic structures, such as are the road infrastructures, which are expected to be self-diagnostic ones for performing efficiently also in post-earthquake emergencies.

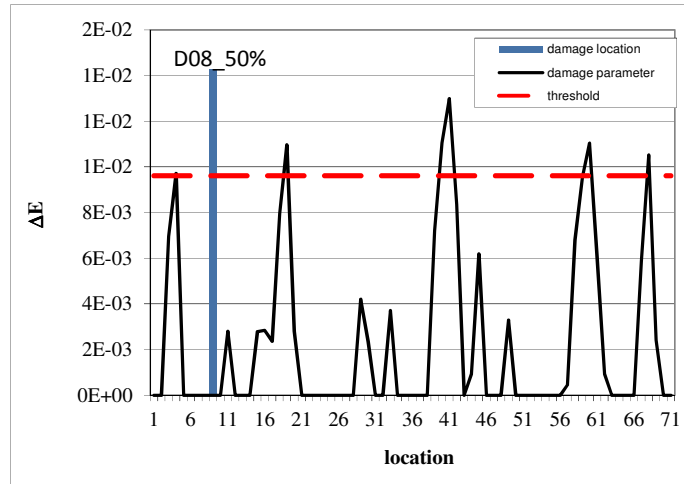


**Figure 5.1.** Results for the IDDM method with sensors of type HN for damage simulated through a 50% stiffness reduction at node N8.

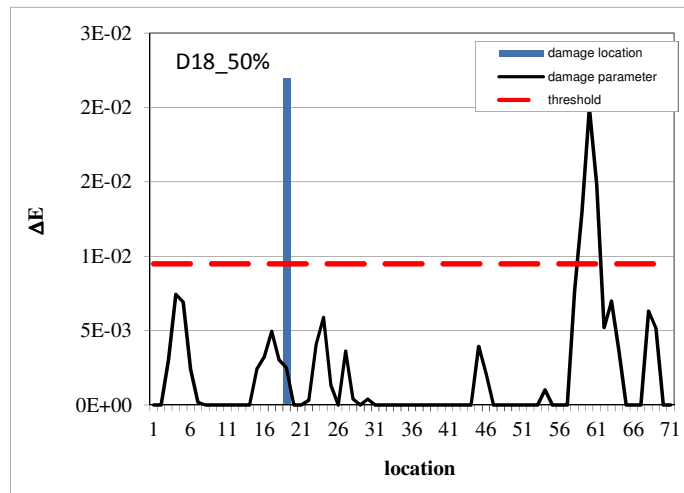


**Figure 5.2.** Results for the IDDM method with sensors of type HN for damage simulated through a 50% stiffness reduction at node N18.

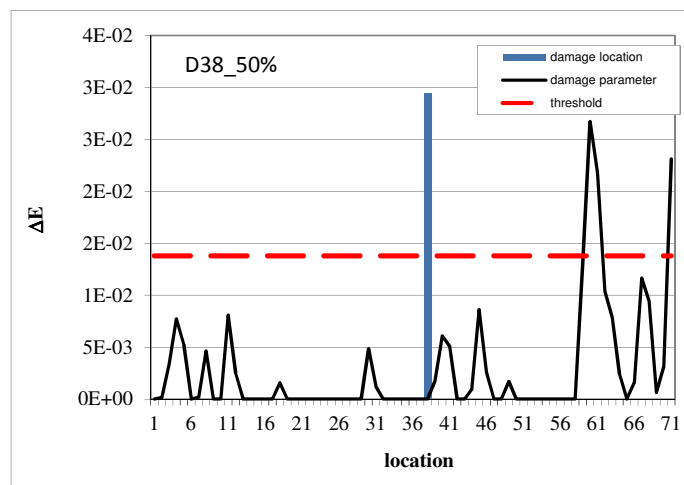


**Figure 5.3.** Results for the IDDM method with sensors of type HN for damage simulated through a 50% stiffness reduction at node N38.



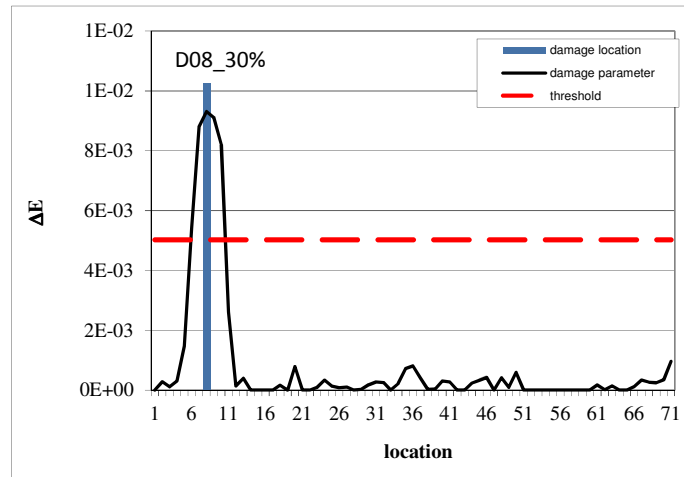


**Figure 5.4.** Results for the IDDM method with sensors of type LN for damage simulated through a 30% stiffness reduction at node N8.

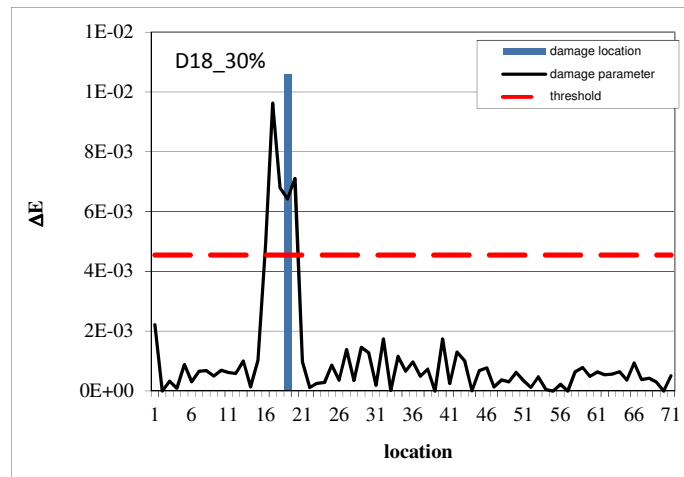


**Figure 5.5.** Results for the IDDM method with sensors of type LN for damage simulated through a 30% stiffness reduction at node N18.

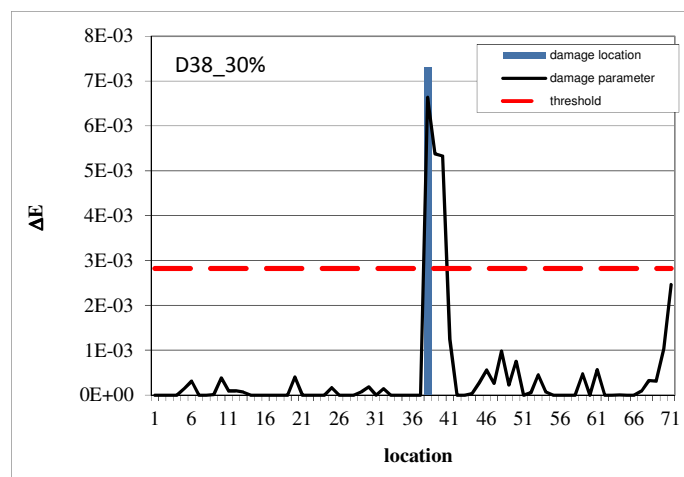


**Figure 5.6.** Results for the IDDM method with sensors of type LN for damage simulated through a 30% stiffness reduction at node N38.

## ACKNOWLEDGEMENTS

This work has been partially supported by MIUR (Ministry of Education, University and Research) under the project "Dynamic response of linear and nonlinear structures: modelling, testing and identification" (PRIN 2009).

## REFERENCES

- Allemang R.J., Brown D.L. (1982). A Correlation Coefficient for Modal Vector Analysis. *Proc. 1st International Modal Analysis Conference (IMAC)*, 110-116.
- Domaneschi M., Martinelli L. (2011). Optimal passive and semi-active control of a wind excited suspension bridge. *Structure and Infrastructure Engineering: Maintenance, Management, Life-Cycle Design and Performance*. 1-18, DOI:10.1080/15732479.2010.542467, Available online: 04 Jan 2011.
- Domaneschi M., Limongelli M.P., Martinelli L. (2011). Wind Driven Damage Detection On A Suspended Bridge. *Proc. Experimental Vibration Analysis for Civil Engineering Structures (EVACES)*. Varenna (Italy), 383 – 390.
- Kho B.H., Dyke S.J. (2007). Structural health monitoring for flexible bridge structures using correlation and sensitivity of modal data. *Computers and Structures*. **85**: 117-130.
- Limongelli M.P. (2009). A damage detection approach based on responses interpolation. *IOMAC Conference*. Portonovo, IT.
- Limongelli M.P. (2010). Frequency Response Function Interpolation for Damage Detection under Changing Environment. *Mechanical Systems and Signal Processing*. **24**: 2898-2913.
- Limongelli, M.P., (2011). The interpolation damage detection method for frames under seismic excitation. *Journal of Sound and Vibration*, 330. 5474–5489.
- Ntotsios, E., Papadimitriou, C., Panetsos, P., Karaiskos, G., Kyriakos P., Perdikaris, P.C. (2009). Bridge health monitoring system based on vibration measurements. *Bulletin of Earthquake Engineering*. **7**: 469-493.
- Pandey A.K., Biswas M., and Samman M.M. (1991). Damage Detection from Changes in Curvature Mode Shapes. *Journal of Sound and Vibration*, **145**: 321–332.
- Ratcliffe C.P. (2000). A frequency and curvature based experimental method for locating damage in structures. *Journal of Vibration and Acoustics*. **122**: 324–329.
- Romano M. (2009). Ponti Sospesi: Controllo sotto azioni eoliche, MSc Thesis, Politecnico di Milano, Milano, Italy (in Italian).
- Sampaio R.P.C., Maia N.M.M. and Silva J.M.M. (1999). Damage detection using the frequency response function curvature method. *Journal of Sound and Vibration*. **226**: 1029 1042.